The Effect of Transformation Temperature and Holding Time of Bainite Structure Formation on S45C Steel

Wahyuaji Narottama Putra
Department of Metallurgy & Materials, Faculty of Engineering, Universitas Indonesia

Mochamad Iqbal Adha Widjana
Department of Metallurgy & Materials, Faculty of Engineering, Universitas Indonesia

Anis, Muhammad
Department of Metallurgy & Materials, Faculty of Engineering, Universitas Indonesia

Prasetyo, Yus
Department of Metallurgy & Materials, Faculty of Engineering, Universitas Indonesia

https://doi.org/10.5109/6625732

出版情報：Evergreen. 9 (4), pp.1218-1223, 2022-12. 九州大学グリーンテクノロジー研究教育センター
バージョン：

The Effect of Transformation Temperature and Holding Time of Bainite Structure Formation on S45C Steel

Wahyuaji Narottama Putra[1*], Mochamad Iqbal Adha Widjana[1], Muhammad Anis[1], Yus Prasetyo[1]
[1]Department of Metallurgy & Materials, Faculty of Engineering, Universitas Indonesia

*Author to whom correspondence should be addressed:
E-mail: wahyuaji@ui.ac.id

(Received February 11, 2022; Revised December 25, 2022; accepted December 25, 2022).

Abstract: Nowadays, many applications are utilizing bainite as, for instance, lightweight design of car bodies. Bainite phase has higher hardness compared with ferrite, pearlite and austenite, but still retain better toughness than martensite. To create a bainite, however, a specific method called austempering is needed where the steel is quenched in the temperature below pearlite formation and held for a certain time. The optimalization of the quench temperature and holding time become very important. In this study, series of heat treatment processes have been carried out on the S45C steel to form bainite structure. The heat treatment processes include variations of transformation temperature from 200 – 400°C, and holding time from 1 – 5 hours, The lower salt-bath temperature and longer holding time generated larger amounts of bainite. In average, the highest hardness result was achieved on 5 hours holding time at 200°C with 42 HRC, and the lowest hardness was on 1 hour holding time at 400°C with 22 HRC.

Keywords: Bainitic steel, Bainite microstructure, S45C carbon steel, Salt bath

1. Introduction

Steel is a material consist of iron and carbon. Other elements such as chromium, manganese, and nickel are added to improve the strength or as well as other steel properties [1)]. Steel has great formability and durability, good tensile and yield strength, and also good thermal conductivity. These properties provide varies of steel usage from structural building to biomaterials [2)].The properties of steel depend on the microstructure and phases. Other solutes whether by design or as impurities may also affect the properties [3)]. The phase in steel can be appeared as austenite, ferrite, cementite, pearlite, bainite and martensite. These different phases depend on carbon content heat treatment process and cooling rate [4)]. Bainite is formed at cooling rates slower than martensite, and faster than ferrite - pearlite formation. Bainitic microstructures offer the best balance between strength and ductility, compared with martensite phase which has very high hardness. Very hard materials tend to difficult to be machined or may need specialized machining process [5–7)]. The cooling rate of bainitic formation is fast enough to increase the strength without producing brittleness. The strength - toughness balance is the reason why an increasing number of automotive components are being made from bainitic steels [8,9)]. Additionally, bainitic steel is not a substitute for wear resistance materials, and many other materials have been studied for this specific usage [10,11)]. For steel-based materials, surface hardening process is more suitable for wear resistance purpose [12)].

Austempering is a process to produce bainitic phase. In this process, the steel is rapidly cooled from the austenitizing temperature to the heat extracting medium, usually molten salt [13–15)]. The molten salt is held at a defined temperature range between 200°C and 400°C. In this temperature range, transformation of austenite into bainite is occurred. The process is commonly used in the automotive industry and other parts where optimum durability formability and durability are necessary [16)]. Holding time is induced to ensure temperature uniformity across all its entire volume [17)]. After holding in higher temperature, the parts are cooled to room temperature accordingly. The final mechanical properties of austempered steel rely upon microstructural parameters such as morphology of bainite or ferrite, volume percentage of retained austenite, and martensite [18)]. Hence, it is a very crucial aspect to determine the most optimal temperature and holding time during quenching in the molten salt.

A salt bath is used widely in austemper process as the molten salt, to extract heat at higher temperature. A nitrate-based is chosen, due to suitable for quenching from austenization temperature up to 900°C. This molten salt is applicable for most carbon and low-alloy steels [19)]. Mixtures of sodium nitrate and sodium nitrite are usually used at lower temperatures for rapid cooling.

2. Experimental Methods

The material used in this study is a medium carbon S45C steel. The composition of this steel is shown on Table 1. Figure 1 shows the microstructure of the S45C steel before any heat treatment. It can be seen from the figure that the main phases in the steel were ferrite and pearlite. The austenization temperature was the same for all sample at 900°C. Meanwhile the salt-bath temperature and holding time were varied at 200 – 400°C and 1 – 5 hours respectively. Both austenization and salt-bath treatment were conducted in Nabertherm Furnace.

The tools used for austemper process were furnaces (for austenization and salt-bath), 60mm-diameter graphite crucible to contain the molten salt, nitrite and nitrate salt. Some of these tools were shown in Figure 2. In this study, the ratio for nitrate and nitrite salt was 1:1. Hardness testing method was used to observe the mechanical properties of the bainitic steel. Rockwell hardness method was done as macro hardness test. For the Rockwell test, 10 kgf minor load and 150 kgf mayor load was used. Additionally, micro-Vickers was done to check the different colored phase in the microstructure. Both hardness testing was done in Center for Materials Processing and Failure Analysis, Faculty of Engineering Universitas Indonesia, using QualiRock Digital Hardness Testers based on ASTM E18-11 standard.

Table 1. Chemical composition of S45C.

Element	% Weight
Carbon	0.47
Silicon	0.27
Manganese	0.7
Phosphorous	0.01
Sulphur	0.006
Chrome	0.25
Aluminum	0.023

Metallography is a versatile method, which can be used to determines the physical structure, chemical composition, and characteristics of the material. Other than observing shapes and structure, metallography is also used to assess the specific characteristics of microstructure through quantitative measurements of microstructure or commonly referred to as quantitative metallography [20]. In this study, metallography was done to analyze the phase and microstructure of S45C steel after heat treatment. Metallography testing was conducted in Technology of Microstructure Analysis Laboratory, Metallurgy & Materials Engineering Universitas Indonesia, based on ASTM E3-11 by using "Precise" grinding and polishing machine. Each specimen was cut into one-centimeter-thick half-rod shape and were mounted by using castable resin method. All specimens were etched with Nital acid, and observed with Carl Zeiss Primotech optical microscope.

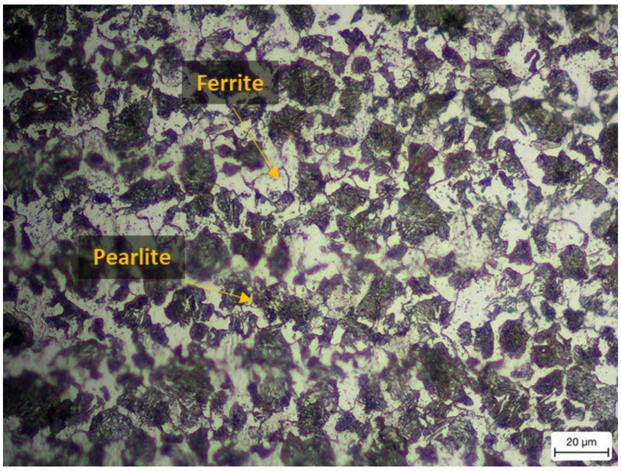

Fig. 1: Micrograph of S45C Steel before Heat Treatment (mag. 500X)

Fig. 2: (a) Sodium Nitrite, (b) Sodium Nitrate, (c) Graphite Crucible, (d) S45C Sample

3. Results and Discussions

The result and discussion section in this paper is divided into several parts i.e., hardness result, microstructure analysis on each austemper temperature, and phase distribution result. Table 2 showed the coding of each sample related with the austempering condition. This coding was used to simplify the discussion.

Table 2. Sample code for each austempering condition

Sample Code	Salt bath Temperature (°C)	Holding Time (hours)
200H1	200	1
200H3	200	3
200H5	200	5

300H1	300	1
300H3	300	3
300H5	300	5
400H1	400	1
400H3	400	3
400H5	400	5

3.1 Hardness result

According to hardness value average, the hardness number increase significantly followed by extended holding time. For example, sample 200H1 produced 26.34 HRC for 1 hour holding time, and 37.52 HRC was produced by sample 200H3 on 3 hours holding time. Meanwhile, sample 200H5 with 5 hours holding time, which was the longest compared to others, had the greatest hardness value with 42.15 HRC. This hardness number was also the highest of all sample even in different austempering temperature. In general, the hardness value can be seen in Figure 3 as the result of all heat treatment processes.

Every group of salt-bath temperature tends to increase in hardness value with longer austempering holding time. These phenomena indicated the formation of different phase in microstructure. For example, if there was a martensite or bainite in the microstructure due to longer holding time, the hardness value was increased significantly [21]. In this research, the carbon content of S45C steel was in between 0.42-0.48 % Carbon. Therefore, it can be assumed that the maximum bainite hardness of this research was below 45 HRC.

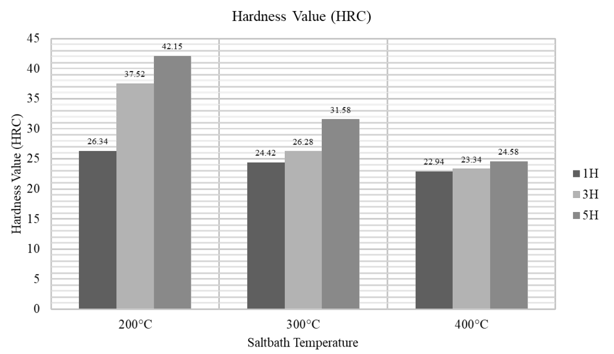

Fig. 3: Rockwell hardness for all samples

Vickers microhardness value from different phase as shown in Table 3 obtained using 100 gf load within 10 seconds. The microhardness testing was conducted on 5 indentations of two appeared phases, white-colored phase and black-clored phase according to Figure 4. The standard used in Vickers microhardness testing was ASTM E384 with MicroMet® 5100 Series Microindentation Hardness Testers testing machine. Indentation number 1 and number 2 which had white phase mark generated 411 HV 0.1, while indentation number 2 to 5 marked by black phase on the microstructure exhibited minimum of 451 HV 0.1.

The testing was done to ensure the different microstructures and phases in this research. The phases present was usually consisting of martensite, bainite, pearlite, and proeutectoid ferrite [22]. The darker phase, normally martensite and bainite, has higher hardness value than the brighter phase which was proeutectoid ferrite.

Table 3. Hardness comparison on different phases

Austempering condition	Vickers Hardness	Phase Color
200°C, 5 hours	410	White
	411	White
	451	Black
	464	Black
	452	Black

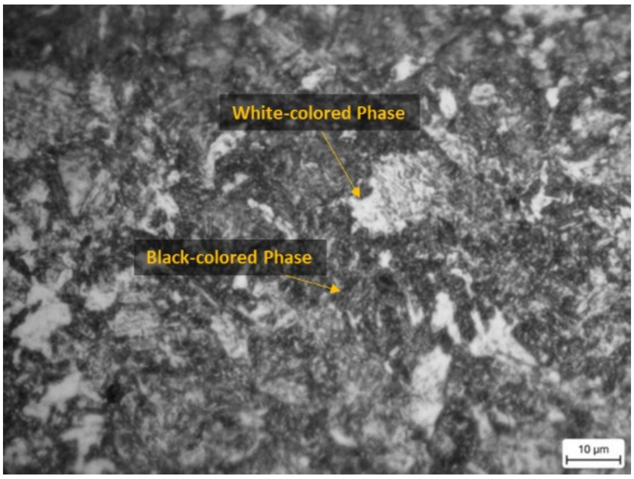

Fig. 4: Identification of different phases for microhardness testing (Mag. 1000X)

3.2 Microstructure analysis on 200°C austempering temperature

Proeutectoid ferrite, lower bainite, and martensite were appeared on sample 200H1. The microstructures were shown in Figure 5 a-c. Proeutectoid ferrite could be formed in the steels if the carbon content was lower than the eutectoid composition. This kind of steel was called hypoeutectoid steels. The formation of proeutectoid ferrite might occurred during the transfer of sample from austenitizing furnace into salt-bath furnace. There was some delay time, hence the transformation from austenite did not directly change into bainite formation [23]. Instead, it reached ferrite nose on TTT diagram before reach bainite start.

3.3 Microstructure analysis on 300°C austempering temperature

Sample 300H1 resulted a proeutectoid ferrite and lower bainite as represented in Figure 5 d-f. Sample 300H1 had different salt-bath temperature compared to sample 200H1, sample 200H3, and sample 200H5. The proeutectoid ferrite were more spread out in the surface compared with 200°C bath. Microstructure in sample

300H5 shows three different constituents: pearlite, proeutectoid ferrite, and lower bainite. The pearlite in sample 300H5 was very clearly visible compared to sample 300H1 and sample 300H3, shown in Figure 6. Pearlite phase was identified by the mutual growth of ferrite and cementite (Fe_3C) from austenite. This resulted in the formation of a lamellar structure that tends to consist of alternating layers of ferrite and cementite in two-dimensional portions.

3.4 Microstructure analysis on 400°C austempering temperature

The main difference of 400°C austempered sample was on the proeutectoid ferrite. In the figure 5 g-i, the proeutectic ferrite appeared wider and bigger on the microstructure. Moreover, there was upper bainite which consists of coarse bainitic, ferrite and austenite with precipitated carbides took place on microstructure. Upper bainite developed at higher temperatures specifically 550–400°C, allowing excess carbon to separate before precipitating in the ferrite [24)].

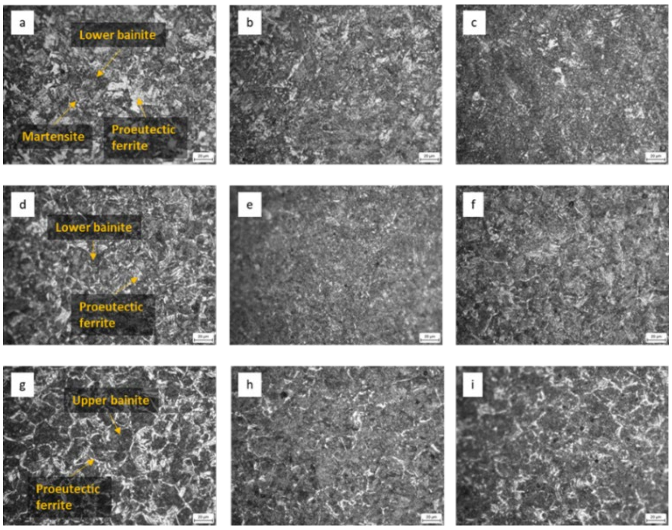

Fig. 5: (a-c) sample 200H1, 200H3, 200H5; (d-f) sample 300H1, 300H3, 300H5; (g-i) sample 400H1, 400H3, 400H5. Scale bar: 20µm

3.5 Phase distribution calculation

Phase distribution was conducted to support the microstructure result obtained by metallography. The calculation was done by using ImageJ application, which is widely used for phase fraction calculation [25,26)]. As the microstructure consists of several phases, some assumption was used for calculation in ImageJ. The white phase indicated a proeutectoid ferrite, meanwhile the black phase usually revealed lower bainite and upper bainite. The remainder phase commonly the grey or lighter black was considered as martensite and pearlite in depending on the temperature. Table 5 shows the distribution of phase percentage according to the appeared microstructures. From the table, it can be seen at 200°C the longer holding time shows more bainite and less proeutectoid ferrite, hence the higher hardness. Higher austempering temperature resulted in pearlite formation, lowering the overall hardness. This result was relevant with the previous discussion [18)]. The composition of the bainite and other phases were strongly dependent with the quench temperature and holding time.

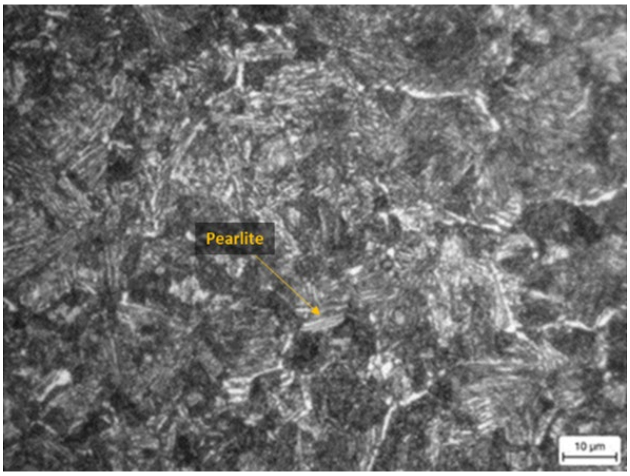

Fig. 6: Pearlite Phase in Sample 300H5

Table 5. Distribution of each phase in different austempering temperature

		Phases			
Sample	Martensite	Lower Bainite	Upper Bainite	Pearlite	Proeutectoid Ferrite
200H1	23.639%	59.498%			16.863%
200H2	28.925%	60.047%			11.028%
200H5	16.99%	77.241%			5.769%
300H1		58.767%		23.043%	18.190%
300H3		60%		22.421%	17.579%
300H5		61.556%		22.586%	15.858%
400H1			53.628%	21.526%	24.846%
400H3			54.680%	24.464%	20.856%
400H5			59.982%	22.167%	17.851%

4. Conclusions

The variation of salt-bath temperature and holding time influenced the appeared microstructure and hardness value on S45C steel. The lower salt-bath temperature showed harder microstructure (martensite and bainite) formation. Martensite and bainite were formed due to the low austempering temperature according to time-temperature transformation diagram. Longer austempering holding time ensure temperature uniformity across all its entire volume, increasing the percentage of bainite which later affecting the hardness value of samples. Meanwhile, higher austempering temperature resulted in the formation of pearlite phase, decreasing the overall hardness number.

Acknowledgements

The author would like to acknowledged the financial support from Hibah PUTI 2020 funded by DRPM Universitas Indonesia No. NKB-2472/UN2.RST/HKP.05.00/2020

References

1) H. Cano, I. Díaz, D. de la Fuente, B. Chico, and M. Morcillo, "Effect of cu, cr and ni alloying elements on mechanical properties and atmospheric corrosion resistance of weathering steels in marine atmospheres of different aggressivities," *Materials and Corrosion*, **69** (*1*) 8–19 (2018). doi:10.1002/maco.201709656.
2) J. Triyono, R. Rahajeng, and E. Surojo, "Surface modification and hardness behavior of aisi 304 as an artificial hip joint using ammonia and scallop shell powder as a nitriding agent," *Evergreen*, **8** (*2*) 335–343 (2021). doi:10.5109/4480714.
3) A.M. Stolyarov, M.V. Potapova, and M.G. Potapov, "Non-metallic impurities in continuous cast billets," *MSF*, **989** 411–416 (2020). doi:10.4028/www.scientific.net/MSF.989.411.
4) E.B. Fredj, H.G. Nanesa, D. Shahriari, J.-B. Morin, and M. Jahazi, "Effect of Cooling Rate on Phase Transformation and Microstructure Evolution in a Large Size Forged Ingot of Medium Carbon Low Alloy Steel," in: T.M. Tms Metals &. Materials So (Ed.), TMS 2017 146th Annual Meeting & Exhibition Supplemental Proceedings, Springer International Publishing, Cham, 2017: pp. 413–423. doi:10.1007/978-3-319-51493-2_39.
5) Ainur Munira Rosli, Ahmad Shahir Jamaludin, and Mohd Nizar Muhd Razali, "Recent study on hard to machine material – micromilling process," *Evergreen*, **8** (*2*) 445–453 (2021). doi:10.5109/4480727.
6) N. Talib, Nor Athira Jamaluddin, Tan Kai Sheng, Lee Woon Kiow, H. Abdullah, S. Ahmad, and A. Saleh, "Tribological study of activated carbon nanoparticle in nonedible nanofluid for machining application," *Evergreen*, **8** (*2*) 454–460 (2021). doi:10.5109/4480728.
7) A. Jain, Cheruku Sandesh Kumar, and Y. Shrivastava, "Fabrication and machining of metal matrix composite using electric discharge machining: a short review," *Evergreen*, **8** (*4*) 740–749 (2021). doi:10.5109/4742117.
8) R.V.S.M. Ramakrishna, K.B. Sankara Rao, G.M. Reddy, and J.P. Gautam, "Friction stir welding of advanced high strength (bainitic) steels for automotive applications," *Materials Today: Proceedings*, **5** (*9*) 17139–17146 (2018). doi:10.1016/j.matpr.2018.04.122.
9) C. Hofer, V. Bliznuk, A. Verdiere, R. Petrov, F. Winkelhofer, H. Clemens, and S. Primig, "High-resolution characterization of the martensite-austenite constituent in a carbide-free bainitic steel," *Materials Characterization*, **144** 182–190 (2018). doi:10.1016/j.matchar.2018.07.011.
10) Shashi Prakash Dwivedi, M. Maurya, and Shailendra Singh Chauhan, "Mechanical, physical and thermal behaviour of sic and mgo reinforced aluminium based composite material," *Evergreen*, **8** (*2*) 318–327 (2021). doi:10.5109/4480709.
11) Anthony Chukwunonso Opia, Mohd Kameil Abdul Hamid, S. Syahrullail, Charles A. N. Johnson, Abu Bakar Rahim, and Mohammed B. Abdulrahman, "Nano-particles additives as a promising trend in tribology: a review on their fundamentals and mechanisms on friction and wear reduction," *Evergreen*, **8** (*4*) 777–798 (2021). doi:10.5109/4742121.
12) J. Liu, C. Ye, and Y. Dong, "Recent development of thermally assisted surface hardening techniques: a review," *Advances in Industrial and Manufacturing Engineering*, **2** 100006 (2021). doi:10.1016/j.aime.2020.100006.
13) H. Mousalou, S. Yazdani, B. Avishan, N.P. Ahmadi, A. Chabok, and Y. Pei, "Microstructural and mechanical properties of low-carbon ultra-fine bainitic steel produced by multi-step austempering process," *Materials Science and Engineering: A*, **734** 329–337 (2018). doi:10.1016/j.msea.2018.08.008.
14) V.A. Alza, "Isothermal treatment at low temperatures applied to aisi 4340 steel: effects on hardness, toughness and microstructure," *IJRTE*, **9** (*1*) 2241–2250 (2020). doi:10.35940/ijrte.A2722.059120.
15) S. Sharma, B.M. Gurumurthy, U.A. Kini, A. Hegde, and A. Patil, "Mechanical characteristics evaluation of dual phase and related hardening techniques on aisi 4340 steel," *JMES*, **12** (*4*) 4018–4029 (2018). doi:10.15282/jmes.12.4.2018.03.0349.
16) P.V. Krishna, R.R. Srikant, M. Iqbal, and N. Sriram, "Effect of austempering and martempering on the properties of aisi 52100 steel," *ISRN Tribology*, **2013** 1–6 (2013). doi:10.5402/2013/515484.
17) S. Ebner, C. Suppan, R. Schnitzer, and C. Hofer, "Microstructure and mechanical properties of a low c steel subjected to bainitic or quenching and partitioning heat treatments," *Materials Science and Engineering: A*, **735** 1–9 (2018). doi:10.1016/j.msea.2018.08.026.
18) L. Lan, M. Yu, and C. Qiu, "On the local mechanical properties of isothermally transformed bainite in low carbon steel," *Materials Science and Engineering: A*, **742** 442–450 (2019). doi:10.1016/j.msea.2018.11.011.
19) B.M. Gurumurthy, S.S. Sharma, and A. Kini, "Ferrite-bainite dual phase structure and mechanical characterization of aisi 4340 steel," *Materials Today: Proceedings*, **5** (*11*) 24907–24914 (2018). doi:10.1016/j.matpr.2018.10.290.
20) V. García-García, I. Mejía, and F. Reyes-Calderón, "Quantitative metallographic characterization of

welding microstructures in ti-containing twip steel by means of image processing analysis," *Materials Characterization*, **147** 1–10 (2019). doi:10.1016/j.matchar.2018.10.012.

21) A. Kumar, S.B. Singh, and K.K. Ray, "Influence of bainite/martensite-content on the tensile properties of low carbon dual-phase steels," *Materials Science and Engineering: A*, **474** (*1–2*) 270–282 (2008). doi:10.1016/j.msea.2007.05.007.
22) Y. Luo, J. Peng, H. Wang, and X. Wu, "Effect of tempering on microstructure and mechanical properties of a non-quenched bainitic steel," *Materials Science and Engineering: A*, **527** (*15*) 3433–3437 (2010). doi:10.1016/j.msea.2010.02.010.
23) S.S. Babu, S. Vogel, C. Garcia-Mateo, B. Clausen, L. Morales-Rivas, and F.G. Caballero, "Microstructure evolution during tensile deformation of a nanostructured bainitic steel," *Scripta Materialia*, **69** (*11–12*) 777–780 (2013). doi:10.1016/j.scriptamat.2013.08.026.
24) M. Azuma, N. Fujita, M. Takahashi, T. Senuma, D. Quidort, and T. Lung, "Modelling upper and lower bainite trasformation in steels," *ISIJ Int.*, **45** (*2*) 221–228 (2005). doi:10.2355/isijinternational.45.221.
25) W. Li, and X. Xue, "Effects of silica addition on chromium distribution in stainless-steel slag," *Ironmaking & Steelmaking*, **45** (*10*) 929–936 (2018). doi:10.1080/03019233.2017.1412386.
26) H.J. Bang, T.G. Le, J.Y. Kim, H.K. Ryu, and K.B. Yoon, "Quantitative study on area fraction of precipitated carbides of hp40nb steel as a function of service period," *J Mech Sci Technol*, **35** (*9*) 3793–3801 (2021). doi:10.1007/s12206-021-2102-y.